Optimal design for vibration energy harvesters based on quasi-periodic structures

Shakiba Dowlati Milehsara, Najib Kacem, Noureddine Bouhaddi

Optimal design for vibration energy harvesters based on quasi-periodic structures

Shakiba Dowlati, Najib Kacem & Noureddine Bouhaddi

Univ. Bourgogne Franche-Comté, FEMTO-ST Institute,
CNRS/UFC/ENSMM/UTBM, Department of Applied Mechanics, 25000 Besançon, France

E-mail: shakiba.dowlati@femto-st.fr

Abstract.

In this paper, the design of large-scale quasi-periodic Vibration Energy Harvesters (VEH) is optimized to enhance the harvested power of an electromagnetic mode localized structure. This work aims to optimize the output power by employing the energy localization phenomenon in a large-scale periodic configuration by introducing the minimum number of perturbations. The harvested power, number and location of perturbations are among the objectives that need to be optimized. A genetic-based mixed-integer optimization algorithm is used to meet the objective functions within a constraint on the system kinetic energy. Numerical simulations for quasi-periodic systems with 20 and 100 Degrees of Freedom (DOF) are performed. It is shown that the ratio of harvested power increases as the number of perturbations rises and it exceeds 80% of the total output power by perturbing almost one-third of the total DOFs. The proposed methodology is a decision-making aid to provide an optimal design in a generalized quasi-periodic VEH in order to reduce the number of harvesting transducers while providing a significantly high amount of harvested power.

Keywords: Electromagnetic Energy Harvesting, Large-Scale Quasi-Periodic Structure, Vibration Energy Localization, Mixed-Integer Optimization

1. Introduction

Further developments of self-power sensing systems in many applications such as the internet of things, environmental monitoring and healthcare monitoring face a considerable obstacle in the energy supply [1, 2]. Replacing or recharging batteries is costly and complex. Energy harvesting can address this issue by generating electrical power from different ambient energy sources such as light, mechanical vibrations, thermal gradients, radio-frequency waves, and acoustic energy [3]. Among these sources, energy harvesting from vibrations, with the advantages of high abundance in the surrounding environments, sustainability, and stability, is an active area of research.

Vibrations sources are fluid flows, ambient noise, human activities and machine and structure vibrations [4, 5].

The vibration energy must be processed in the mechanical domain and then converted into electrical energy using, e.g., electromagnetic [6], piezoelectric [7] and electrostatic [8] transduction. Among these transduction mechanisms, Electromagnetic Energy Harvesters (EMEH) offer advantages such as no need for external voltage input and significant output power from weak vibration [9]. Electromagnetic transducers work based on generating an electromotive force in a conductive coil by magnetic flux variation, as explained by Faraday's law of induction [10].

Vibration energy harvesting devices deal with a narrow harvesting bandwidth which leads to inefficiencies where energy prevails over a larger bandwidth. Several techniques are proposed to broaden the bandwidth and increase the output power density of these devices. One technique is the hybridization of energy harvesters [11] to simultaneously harvest energy from multi-sources and single-source using two or more transduction mechanisms such as piezoelectric–electromagnetic [12], triboelectric-electromagnetic [13] etc. Therefore, their complementary characteristic of high voltage and high current result in improvement in energy conversion at both high and low frequencies and amplitudes of excitation [13]. This also helps to increase the operating frequency bandwidth, the output power density and their applications in different domains [11]. Another efficient technique is the use of harvesters with self-adaptive architecture where the system continuously adapts its resonance frequency to the excitation frequency to increase the output power and widen the operational frequency bandwidth. [14, 15]. Nonlinearity enhanced mechanism is also used to overcome the issue of a narrow frequency bandwidth in the conventional linear-type energy harvesters [16, 17] to modify the resonance behavior [18] and to have multi-resonances [19]. Moreover, numerical and experimental studies have shown that a multimodal configuration covers a range of frequencies and thus broadens the effective frequency bandwidth [20, 21]. Subsequently, some studies have recently investigated the favorable effects of using the energy localization phenomenon in a multimodal configuration on the harvested power density of VEH [22, 23]. The energy localization phenomenon indicates that introducing a very small asymmetry to a periodic structure results in the confinement of energy in the perturbed zones [24]. This phenomenon in disordered weakly-coupled periodic structures, discovered by Anderson [25], is used to increase the amplitude of vibration and thus the harvested power.

Furthermore, performing optimizations of the mechanical and electrical characteristics of VEHs has recently drawn much attention. These optimizations have been performed on the harvested power [26], effective bandwidth [27], structures [28, 29], geometries [30, 31], and the electrical circuit [32]. For electromagnetic multi-DOFs VEH, optimization of the exploitation of the geometric nonlinearity and the nonlinear magnetic coupling has been done to increase the harvested power and bandwidth [33]. In addition, for a quasi-periodic system of 5-DOFs, an optimization procedure has been conducted to search for the optimal position for introducing perturbations to the system [34]. In a

generalized large-scale periodic structure consisting of any number of DOFs, an optimal configuration design for perturbing the system increases the harvested output power. This architecture helps to reduce the number of harvesting transducers in terms of coils, and electrical circuits and to avoid the phase problem since they are implemented in the identified perturbed zones rather than all oscillators. Therefore, obtaining an optimal amount of harvested energy with the minimum number of perturbations can be the main idea for utilizing energy localization in the multimodal VEHs. However, to the authors' knowledge, optimization of the required number of perturbed DOFs and the appropriate location for introducing perturbations to a periodic system with any number of DOFs has not been done to improve the power output.

In this paper, the design and performance of a large-scale quasi-periodic electromagnetic VEH of any number of DOFs are optimized in the presence of the energy localization phenomenon. The purpose is to maximize the harvested energy considering the minimum number and appropriate location of perturbed DOFs. A genetic-based mixed-integer optimization algorithm is developed to meet the objectives within a constraint on the kinetic energy criterion. This criterion is introduced to quantify the ratio between the confined kinetic energy in the perturbed zones and the total kinetic energy of the system. The result of the study helps to reduce the cost and size of the device, to overcome technological constraints and to enhance the harvested power density.

2. Design and System Modeling

Figure 1 illustrates a VEH consists of N cantilever beams coupled by magnets at the free end. Magnets are arranged so that there is a repulsive magnetic force between each two adjacent magnets. The oscillators are coupled to a simple electrical circuit via an electromechanical coupling mechanism. With a harmonic base excitation, the relative motion of the magnet masses and coils causes a magnetic flux variation through the coil turns and a current induces in each coil. The generated electrical energy is transferred and dissipated into load resistances [21].

Figure 2 shows N-DOFs discrete system of the harvester. This N-DOF system is an equivalent model of the real VEH that is based on coupled cantilever beam-mass system, depicted in figure 1, in which each cantilever beam with proof mass is represented by one DOF. In this model, m is the equivalent mass of the magnet, k is the mechanical stiffness, x is the relative displacement of each mass, and $\ddot{X}_g = X_g cos(\omega t))$ is the basis-imposed acceleration of the total system where X_g is the imposed acceleration amplitude. Moreover, $c_m = 2\xi_m m\omega_0$ is the mechanical damping of the system in which ξ_m is the mechanical damping coefficient and ω_0 is the eigenfrequency of the decoupled 1-DOF oscillators.

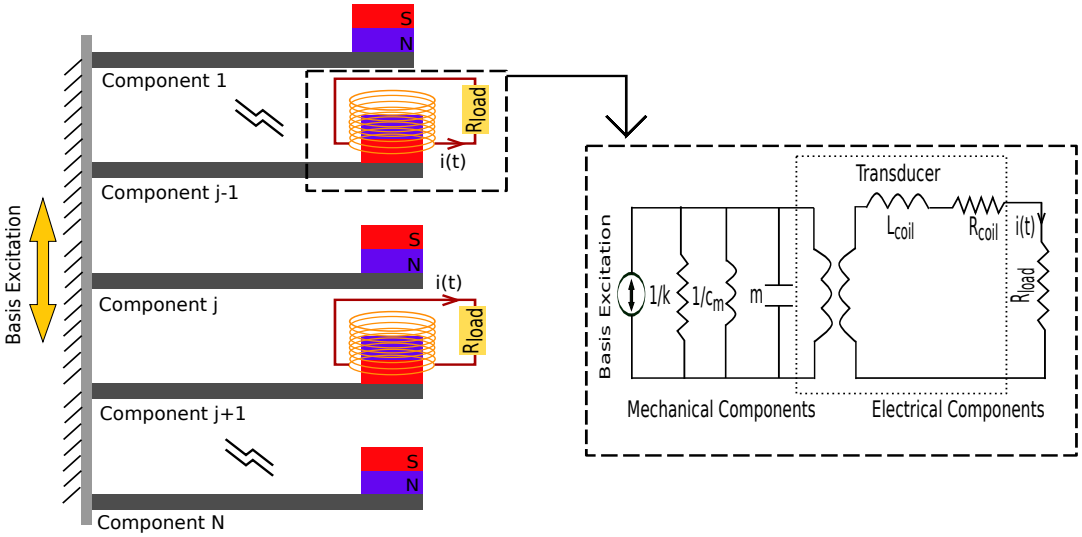

Figure 1: Schematic diagram of the real periodic electromagnetic VEH under harmonic basis excitation consisting of weak-coupled cantilever-beams with moving magnets on the tip where the electromagnetic transduction components are localized on the perturbed DOFs. Equivalent corresponding circuit of the perturbed DOF: the mechanical component is composed of a spring stiffness k, a proof mass m, and a mechanical damping c_m. The electrical component is composed of coil inductance L_{coil}, coil resistance R_{coil}, the load resistance R_{load} , and the induced current in the coils corresponded to the perturbed magnetic mass $i(t)$.

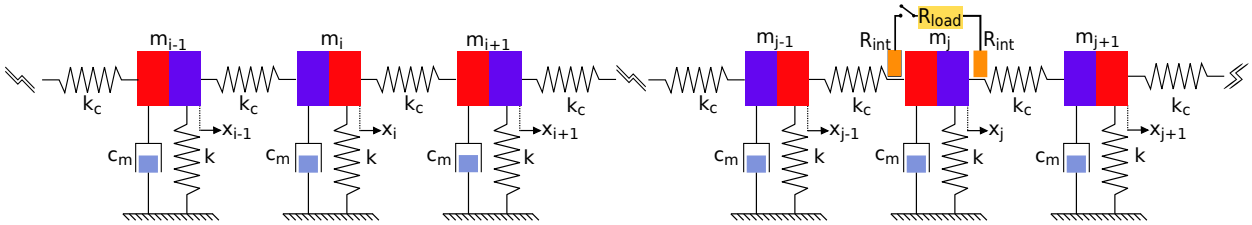

Figure 2: Equivalent N-DOF spring-mass system of the whole electromagnetic VEH where k is the spring stiffness, c_m is the mechanical damping, k_c is the weak coupling stiffness between each two adjacent magnets, R_{int} is the coil internal resistance and R_{load} is the electrical load resistance.

2.1. Equations of Motion

The generalized equation of motions governing the linear behavior of the introduced harvester in figure 2 is expressed based on Newton's 2nd law as

$$\alpha_i \ddot{x}_i + 2\alpha_i \xi_m \omega_0 \dot{x}_i + \omega_0^2 \left[(1+2\beta)\, x_i - \beta x_{i-1} - \beta x_{i+1}\right] = -\alpha_i \ddot{X}_g \tag{1}$$

where α_i is the mistuning parameter and β is the coupling coefficient, defined as follows

$$\alpha_i = \frac{m_i}{m}, \;\; \beta = \frac{k_c}{k} \tag{2}$$

where m_i is the mass of ith DOF and K_c is the linear magnetic stiffness. It is noteworthy that $\alpha_i = 1$ indicates that there is no perturbation in the relevant DOF and $\alpha_i \neq 1$ indicates that the corresponding DOF is perturbed. The electromagnetic transduction

is introduced through a mechanical-magnetic coupling equation as follows

$$\begin{gathered}\alpha_j\ddot{x}_j + 2\alpha_j\xi\omega_0\dot{x}_j + \omega_0^2\left[(1+2\beta)\,x_j - \beta x_{j-1} - \beta x_{j+1}\right] = -\alpha_j\ddot{X}_g \\ V_j + (R_{int} + R_{load})i(t)_j = 0 \\ V_j = \delta_e\dot{x}_j \\ i(t)_j = \frac{\delta}{(R_{load} + R_{int})}\dot{x}_j \end{gathered} \tag{3}$$

where V_j is the induced voltage in the coil, $i(t)_j$ is the induced current in the coil, δ_e is the electromagnetic coupling coefficient, R_{int} and R_{load} are coil internal resistance and load resistance, respectively. Coil inductance L_{coil} is very small and therefore is ignored. In Eq.2, $\xi = \xi_m + \xi_e$ stands for total damping coefficient in which ξ_e and ξ_m are electrical and mechanical damping coefficients, respectively. Electrical damping comes from coils to the system for electromagnetic transduction.
The steady-state response is $x_j = X_j(\omega)\exp^{i\omega t}$ and the instantaneous power absorbed by the electrical damper is $P^j(t) = \frac{1}{2}c_e\dot{x}_j\dot{x}_j^*$ in which $\dot{x}_j^*$ is the conjugate of $\dot{x}_j$ and and $c_e = {\delta_e}^2/(R_{load} + R_{int})$ is the electrical damping. The average harvested power from the j^{th} DOF, in a cycle of vibration, is

$$P_{avr}^j = \frac{c_e\omega^2\left|X_j\right|^2}{2} = \xi_e m_j\omega_0\omega^2\left|X_j\right|^2 \tag{4}$$

The total average power, from all perturbed DOFs can be defined as:

$$P_{avr} = \sum_j P_{avr}^j = \sum_j \xi_e m_j\omega_0\omega^2|X_j|^2 \tag{5}$$

Several methods have been proposed to enhance the performance of VEHs. Among these methods, many numerical and experimental studies have shown that in weakly-coupled quasi-periodic VEH, the amplitude of vibration and thus the output harvested power increases in the perturbed zones. This allows to harvest energy only from perturbed DOFs rather than all of them, and leads to the reduction in the number of transduction circuits.

2.2. Energy Localization

In weakly-coupled periodic systems, introducing any structural mistuning in terms of geometry, added mass, and coupling stiffness breaks the symmetry and results in the confinement of energy and thus strong vibration localization in the perturbed zones [25]. The forced response amplitude of mistuned system is related to the mistuning and coupling coefficients [21]. A 20-DOFs periodic system including an array of weakly-coupled cantilever beams with proof masses on hlthe tip, shown in figure 3a is employed to illustrate the energy localization phenomenon. This system is analyzed by a finite element method. The coupling between two successive cantilever beams is achieved by

a 1D mechanical spring. These couplings are weak ($\simeq$ 1 to 5% of the beam stiffness). Figure 3b shows the first bending mode shape where the kinetic energy of the periodic system is uniformly distributed.

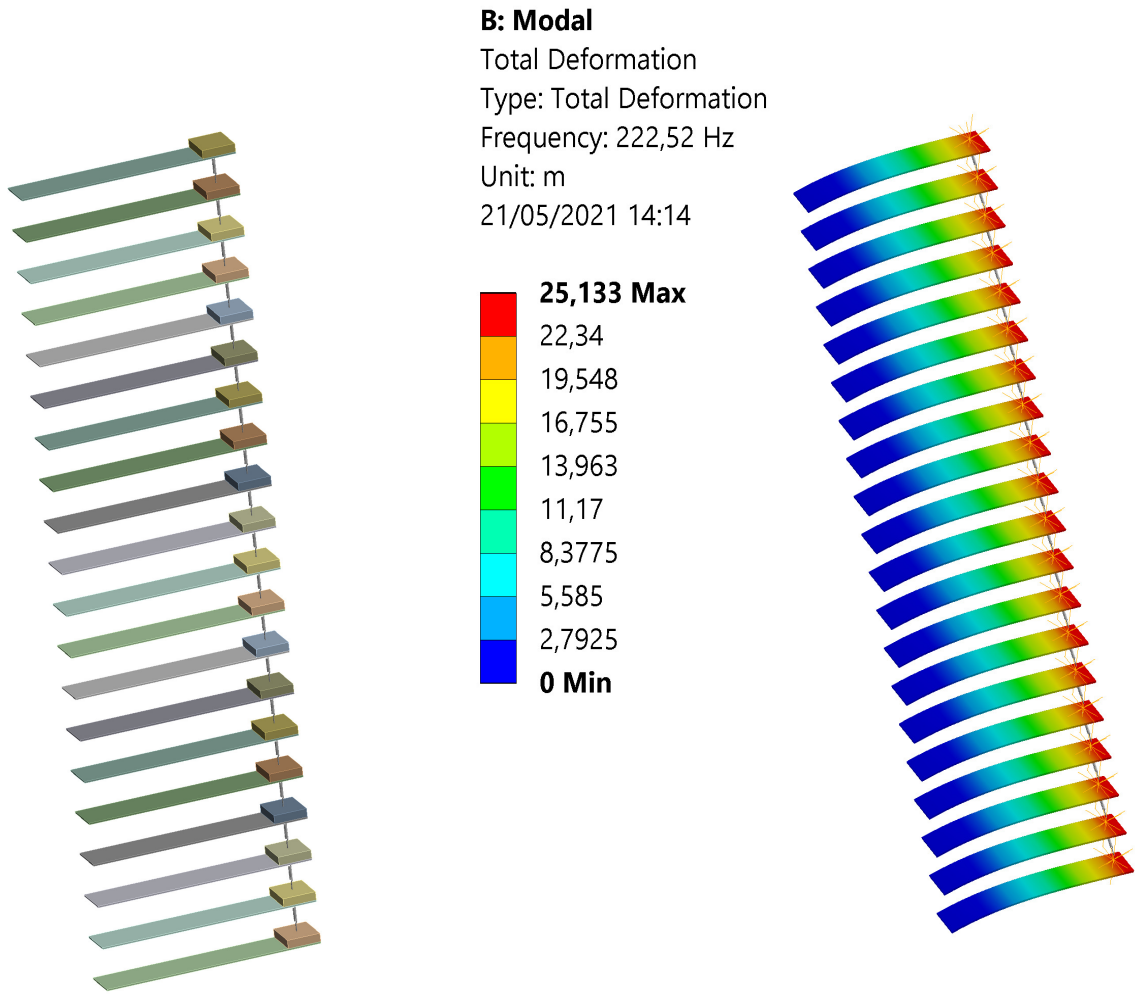

(a) (b)

Figure 3: (a) A periodic system including an array of 20 weakly-coupled cantilever beams with proof masses. The coupling between two successive cantilever beams is achieved by 1D mechanical spring. (b) First bending mode shape of this system

Figure 4 depicts the first bending mode shape of the coupled beam-mass system subjected to the variations in mass density. The perturbation is introduced to the system through variations in mass density by 3% in the $4th$, $11th$ and $17th$ masses (counting from the bottom). The beams with a perturbed mass on the tip noticeably have larger displacements.

It has been discussed that having perturbation in a periodic VEH with many weakly-coupled DOFs causes energy localization in those zones. This phenomenon can be employed in the design of VEHs to decrease the complexity of the device. Therefore,

optimizing the number and the location of perturbations for obtaining the maximum possible harvested power allows for further development in performance of VEHs.

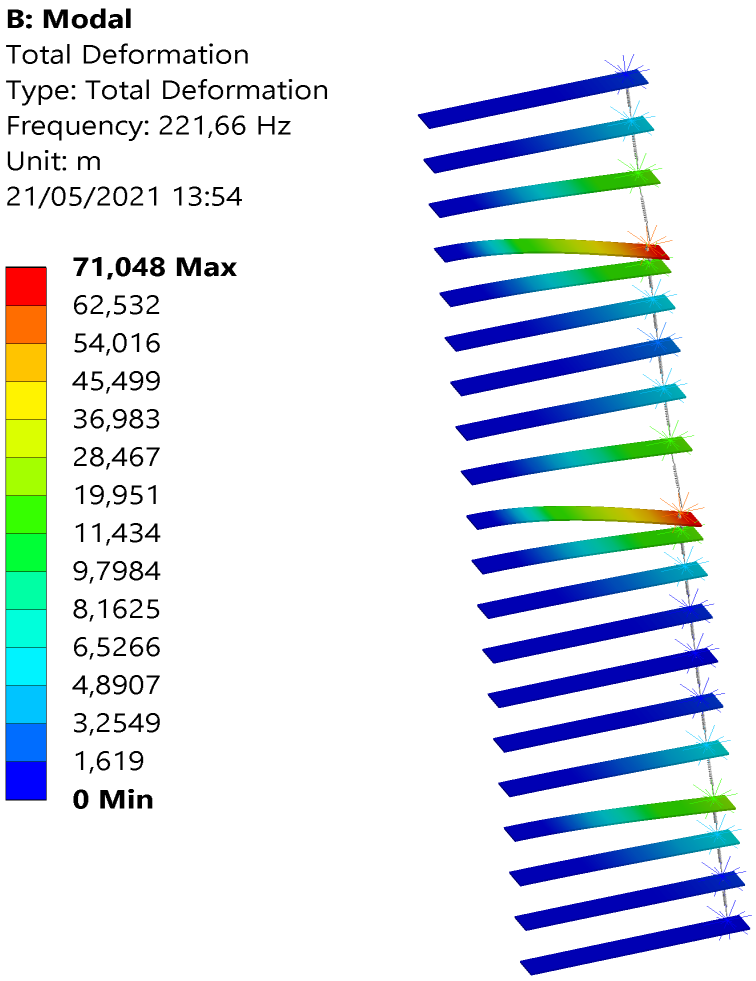

Figure 4: First bending mode shape of a coupled beam-mass system subjected to variations in mass density by 3% in the $4th$, $11th$, and $17th$ mass (counting from the bottom)

3. Optimization procedure

The optimization of the quasi-periodic VEH with many DOFs, shown in figure 2, involves investigating the power output by perturbing certain DOFs in terms of their number and location in a predetermined criterion of kinetic energy. Accordingly, the objective functions are maximizing the harvested power and minimizing the number of perturbed DOFs with specific amount of perturbation. It is also necessary to identify the best DOFs for perturbating the system. A constraint on the criterion of kinetic energy with a predefined amount can also be considered to ensure having a minimum amount of the total kinetic energy in the system. The optimization problem is expressed as

$$\min_{y} (f_1, f_2)$$
$$g(y) = -C_{KE} + E_{min} \leq 0 \tag{6}$$

where f_1 and f_2 are conflicting objective functions, $y = Y(\omega, \xi_e, \alpha)$, $\xi_e = [\xi_{e1}, \ldots, \xi_{ej}, \ldots, \xi_{eN}]$, $\alpha = [\alpha_1, \ldots, \alpha_j, \ldots, \alpha_N]$, C_{KE} is the the criterion of kinetic energy and E_{min} is the value predefined by decision maker. For consistency, the maximization problem $max(-f_1)$ is transformed into an equivalent minimization problem $min(f_1)$. The objective function for maximizing the output harvested power is

$$f_1 = -\sum_{j} \xi_e m_j \omega_0 \omega^2 |X_j|^2 \tag{7}$$

For the second objective function, a binary variable Z_i is assigned to each DOF that reflects perturbation with 1 and lack of perturbation with 0. Therefore, $Z = [Z_1, \ldots, Z_i, \ldots, Z_N]$ is the vector created using the assigned binary values for the whole system. To minimize the number of perturbations, the objective function is expressed as

$$f_2 = \sum_{i=1}^{N} Z_i \tag{8}$$

This objective function not only can determine the number of perturbed DOFs but also identify the best location for perturbing the system. Design variables are continuous for one objective function and discrete for the other, which turns the optimization problem into a mixed-integer problem [35]. Since the optimization problem involves more than one objective function, using multi-objective approach does not seem feasible.Therefore the weighted sum method is used to treat a multi-objective optimization problem as a single-objective one [36]. This single-objective function is a sum of objective functions f_l multiplied by weighting coefficients w_l, formulated as

$$min \sum_{l=1}^{2} w_l f_l \tag{9}$$

in which $w_l \geq 0$ and $\sum w_l = 1$. Weights of each objective function are assigned by the decision-maker based on the intrinsic knowledge of the problem.
Since the objective functions have different magnitudes, their normalization is required for having a consistent solution. Thus, the weights are computed as $w_l = u_l \theta_l$ in which u_l is the weights assigned by the decision-maker and θ_l are the normalization factors. Among different normalization methods, the objective functions are normalized by the maximum value of the objective functions [37]. Therefore, the objective function is

$$min\left(w\frac{f_1}{max\left(f_1\right)}+(1-w)\frac{f_2}{N}\right) \tag{10}$$

in which the maximum value for the f_1 is obtained through the optimization procedure and the maximum amount for f_2 is the total number of DOFs (N), as all the DOFs are perturbed.

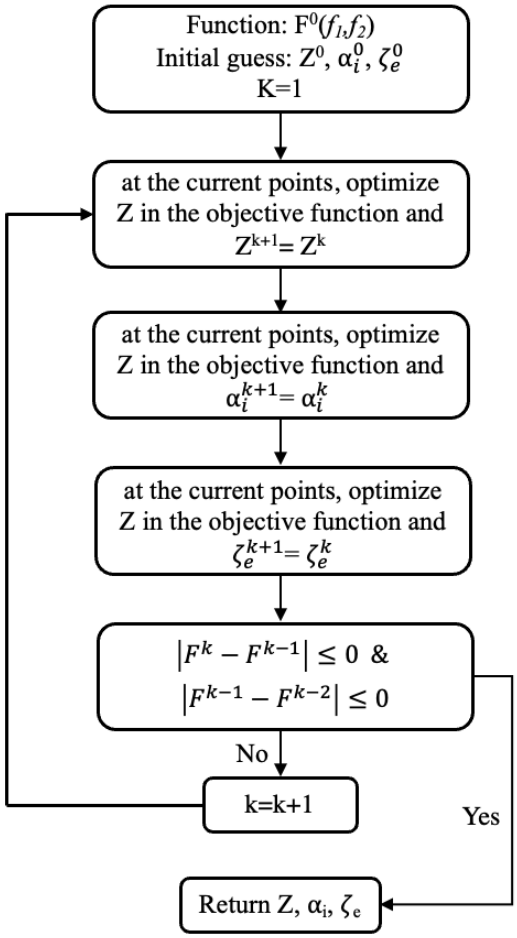

Figure 5: The Flowchart of GA-based algorithm

A constraint (C_{KE}) has been introduced as the criterion of kinetic energy, that is

$$C_{KE}=\frac{\sum_j m_j x_j^2}{\sum_{i=1}^{N} m_i x_i^2} \tag{11}$$

in which i refers to all of the DOFs and j stands for DOFs with perturbation. m and x are the mass and the relative displacement, respectively. Quantitatively, this criterion is the ratio between the sum of the maximum kinetic energy in the perturbed DOFs and the total maximum kinetic energy of the system.

Genetic algorithms (GAs) are general-purpose population-based stochastic search techniques that mimic the principles of natural selection and genetics laid down by

Sivanandam and Deepa [38]. Since continuous and binary values are part of the optimization problem, a genetic-based mixed-integer optimization is used in which the algorithm automatically ensures a gradual shift towards the feasibility of newly generated points. It is also necessary to define a stopping criterion to analyze where the final solutions are obtained and further computation is not required. This criterion ensures the solution is the best acceptable answer, and the results do not change in further iterations. The procedure involved in the GA-based optimization is summarized in figure 5.

4. Results and Discussion

4.1. Numerical simulations

Optimizing the configuration design for quasi-periodic VEH systems with 20 and 100-DOFs is discussed in this section. This study uses the design parameters listed in Table 1, and the objective functions and constraint listed in Table 2. The criterion of kinetic energy is considered more than 0.5 determining the kinetic energy of all of the perturbed DOFs must be at least half of the total kinetic energy of the system. The results that are presented using the Pareto front figures help to find a compromising space between two objective functions (f_1, f_2).

Table 1: Design parameters and functions to be optimized for the corresponding quasi-periodic structure

Constant design parameters	**Design variables**	**Functions to be optimized**
$m = 0.05\ kg$	$\alpha = [\alpha_1, \ldots, \alpha_j, \ldots, \alpha_N]$	Harvested power
$k = 100\ N.m$	$\xi_e = [\xi_{e1}, \ldots, \xi_{ej}, \ldots, \xi_{eN}]$	The total number of perturbed DOF $(\sum_{i=1}^{N} Z_i)$
$\beta = 0.014$		The location of perturbed DOFs
$\xi_m = 0.006$		

Table 2: Objective function and constraints applied in the optimization procedure

Objective function and constraints
$\min(\frac{wf_1}{max(f_1)} + \frac{(1-w)f_2}{N})$
$0.5 \leq C_{KE}$
$1 \leq \alpha_i \leq 1.1$
$0 \leq \ w \leq 1$

Figure 6 shows the ratio of harvested power versus the number of perturbed DOFs for a structure with 20-DOFs. Each point in the figure corresponds to a certain amount of weight (w). $w = 1$ indicates that the optimization procedure is performed only on the harvested power ratio and for the case $w = 0$, only the number of perturbed DOFs is under the optimization procedure. Sweeping w from 1 to 0 considerably changes the optimized value for both harvested power and the number of perturbations. A compromise zone between the two objectives can be selected for extracting the design variables in order to improve the system design and performance. Table 3 lists the output

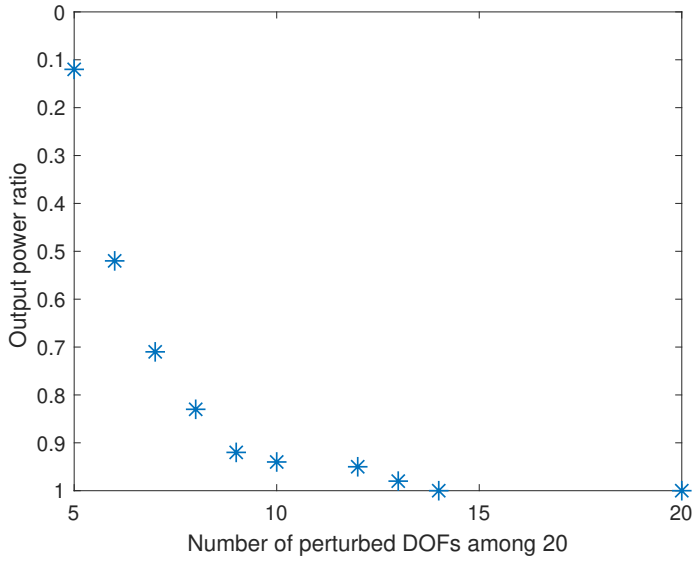

Figure 6: Pareto front of the 20-DOFs system: harvested power versus the number of perturbations

power ratio subjected for the different numbers of perturbations in the structure. For $w = 0$, the value for output power ratio is 0.12 with 5 perturbed DOF for a system of 20-DOFs. As the weight on the (f_1) increases, the number of perturbed DOFs (f_2) increases, and thus both the number of required perturbations and the harvested output power increase. It is shown that perturbing 8 DOFs provides 81% of the total energy of the periodic system. The amounts of harvested power increases as the number of perturbations rises and by perturbing only half of the DOFs, the total output power ratio reaches to more that 90%.

Table 3: Optimized output power ratio for different number of perturbed DOFs

Optimal number and positions of perturbed DOFs among 20	20	13	12	10	8	7	6
Optimized output power in % compared to the total power	100	98	92	91	81	70	52

The Pareto front of the 100-DOFs system is depicted in figure 7 which shows harvested power ratio versus the number of perturbations. As discussed for the 20-DOFs system, different values of weight (w) result in different points in the figure. Similarly, $w = 0$ indicates the situation where the total emphasis is on minimizing the number of perturbed DOFs irrespective of the value for harvested power. As w increases from 0 to 1, the optimal value for each function began to change. This helps to find an optimal zone for extracting the optimal design values. For $w = 1$, the value for output power is 1 which indicates the maximum output power is harvested with expenses of harvesting from all of the DOFs. These numbers for the case $w = 0$ fall into 0.14 for output power and 25 for the number of perturbations. As illustrated, perturbing one-third of DOFs contributes to harvesting more that 80% of the total power.

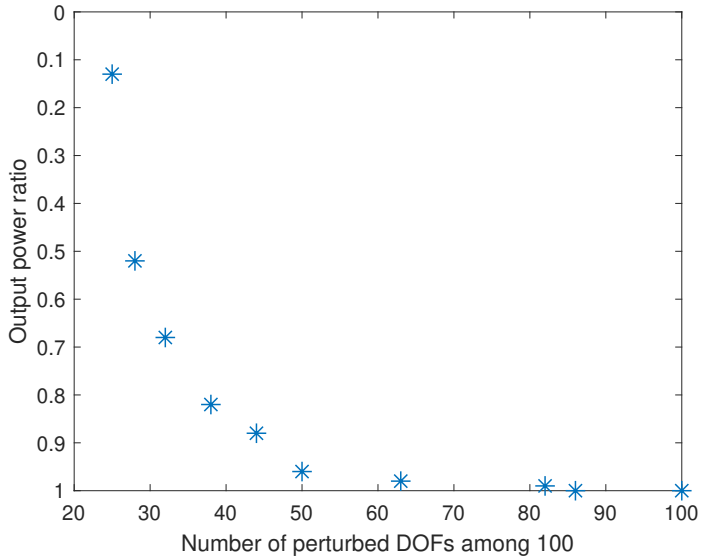

Figure 7: Pareto front of the 100-DOFs system: harvested power versus the number of perturbations

Perturbing any arbitrary combination of DOFs does not necessarily provide the maximum available kinetic energy and thus output power. Table 4 illustrates the criterion of kinetic energy for the case with 5 perturbed DOFs among 20. These DOFs are chosen both randomly and through the optimization procedure and then the criterion of kinetic energy is calculated. It is shown that where the location of perturbation is chosen randomly, the value for the kinetic energy criterion is lower than the constraint defined earlier ($0.5 \leq C_{KE}$). However, locations based on the optimization procedure ensure meeting the defined constraint. It is worth mentioning that there is not one specific optimal set of locations for perturbations and different combinations for perturbations can meet the desired conditions.

Table 4: The criterion of kinetic energy considering different locations of perturbations

Selected method	**Perturbation in DOFs number**	**The criterion of kinetic energy**
Randomly chosen	3 6 8 11 15	0.24
	1 3 8 11 18	0.43
	4 5 12 15 19	0.32
	2 6 8 12 16	0.29
Optimization procedure	2 8 12 17 20	0.52
	2 8 12 16 19	0.51

Potential distribution functions can be adapted to approximate the harvested power ratio regarding the number of perturbed DOFs. This helps to evaluate the goodness of design variables without undergoing an optimization procedure. The harvested power ratio for the case of 8 perturbed DOFs in the 20-DOFs structure is fitted to the distribution function including Normal, Uniform and Exponential. The goodness of fit of the data is listed in Table 5. Results indicate that Normal distribution fits

the data best, as the amount of Kolmogorov-Smirnov and Cramer-von Mises are lower (with $mean = 0.8$ and $standarddeviation = 0.005$). Regarding the test values, the exponential distribution function is not a suitable distribution for this data set at all, and the assumption of following this distribution is rejected.

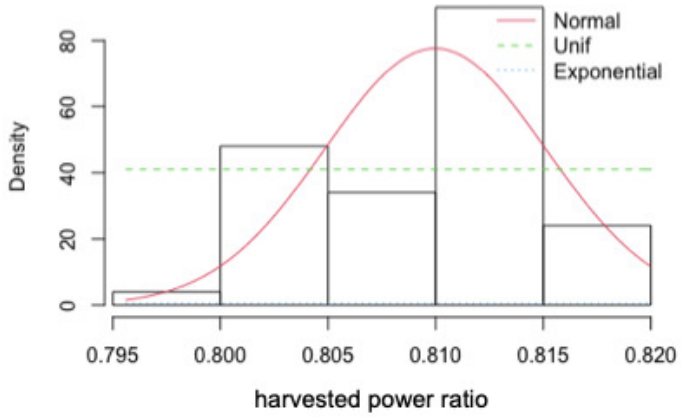

Figure 8: Histogram and distribution functions

Table 5: The goodness of fit of output power with 8 perturbed DOF in 20-DOF structure

Goodness-of-fit statistics	**Normal**	**Uniform**	**Exponential**
Kolmogorov-Smirnov	0.2148220	0.2159016	0.6255302
Cramer-von Mises	0.7890177	1.9175701	9.9499349

Using the optimization procedure, 8 appropriate DOFs among 20 can provide almost 80% of the total power output. To illustrate how the distribution function ensures the goodness of selected variables, 8 random DOF (DOFs number 1,2,4,6,7,8, 16 and 19) are selected to be perturbed and the harvested power ratio is calculated to be 49%. However, the harvested power ratio with perturbing 8 DOFs chosen through the optimization procedure is almost 80%.
Both the amount of output power and the number of perturbations and thus transduction circuits are of great importance in improving the design and performance of the VEH system. It, therefore, is necessary to search for a compromise point where both objectives are recognized to an optimal extent. The optimization procedure is done for a quasi-periodic system of 1000-DOF and the results have shown that perturbing 561 DOFs leads to harvesting almost 94% of the total power.

4.2. Discussion

The Figure of Merit (FoM) is illustrated in figure 9 to study the efficiency of the proposed VEH in comparison with the state of the art of vibration energy harvester. Among different performance metrics, the FoM is calculated by ($FoM = P/Vol.g^2$) where P is the harvested power, Vol is the harvester volume and g is the imposed acceleration

amplitude [45]. The results are calculated theoretically and shown in figure 9. The proposed design provides competitive performance in term of power density and low useful frequency compared to the harvesters based on electromagnetic transduction.

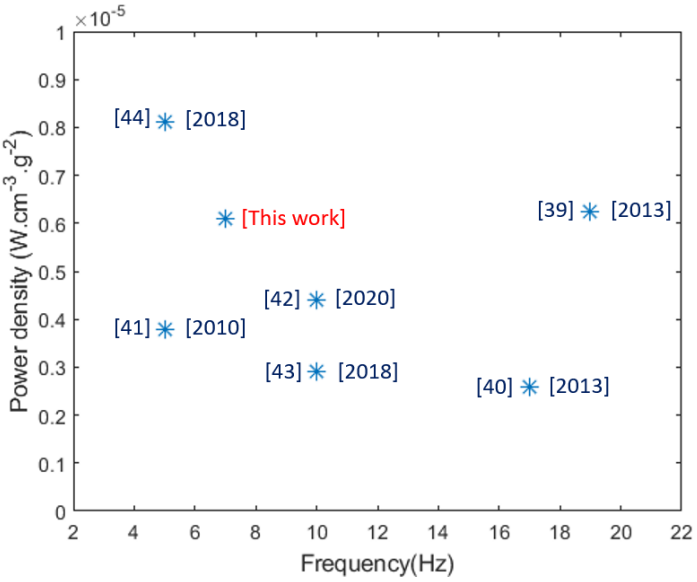

Figure 9: Performance comparison of the proposed optimized VEH FoM with the state-of-the-art

The proposed method is applicable where the building block of VEH is the weakly-coupled identical subsystems such as cantilever beams, clamped-clamped beams, and spiral-shaped springs. This is also feasible in architectures such as levitation-based [21], and free moving ball-based harvesters but their main drawback is the dry friction between moving magnets and the contact area of the guide.

The mistuning can be achieved in periodic systems by perturbing the geometry, mass, and (or) coupling stiffness. For example, magnetic coupling stiffness can be adjusted by tuning the gap between two successive moving magnets [22, 23]. In the proposed study, the mistuning is achieved by the perturbations of some moving magnets.

In terms of energy efficiency, a compromise between the harvested energy and the perturbation level of the localized DOFs is found. As shown in figure 6, 80% of the total energy of the periodic system is harvested while only one-third of the DOFs are perturbed. Currently, the proposed methodology is implemented in the linear VEH where the geometric and magnetic nonlinearities are negligible (low response amplitude and weak coupling). The reason behind this choice is to validate the proof-of-concept in future work. It is recently shown that there is no conflict between the localization phenomenon and nonlinear behavior [23]. Consequently, this methodology can be generalized to the nonlinear VEH in order to both improve the harvested power and the bandwidth.

Experimental investigations will be performed to achieve the proof-of-concept of the proposed methodology. To do so, a periodic 10-DOFs system composed of moving magnets guided by cantilever beams will be fabricated. The device composed of

mechanical structure and electromagnetic transduction will be mounted on a shaker that provides harmonic base acceleration $X_g = 0.1ms^{-2}$. The first eigenfrequency of the periodic structure will be measured by frequency sweep tests. Then, based on the optimization results, three selected DOFs will be perturbed by added masses (less than 10%) on the moving magnets. Vibration energy will be harvested from the three perturbed DOFs with optimal load resistances (R_{load}). Once the model validation step is achieved, it is expected to scavenge almost 80% of the total power for several optimal configurations. To illustrate the performance of the proposed methodology, the experimental results will be compared to random configurations without optimization in terms of positions of perturbed DOFs and mistuning amplitudes.

Conclusion

This paper proposed design optimization for quasi-periodic electromagnetic VEH with many DOFs. The energy localization phenomenon is employed to improve the output power level considering the number of perturbations in DOFs. The energy localization phenomenon is introduced through a finite element method for a 20-DOF quasi-periodic mass-beam system to show how introducing perturbations leads to the confinement of energy and therefore increases the magnitude of vibration in those zones. The optimization procedure is developed to provide the optimal number and location of perturbations for improving the harvested power. It is shown that optimal perturbations in almost one-third of DOFs provide 80% of the total harvested power for VEH of both 20-DOFs and 100-DOFs. Also, perturbing approximately half of DOFs contributes to harvesting more that 90% of the total power. Furthermore, for several arbitrary locations of perturbations, the kinetic energy criterion has been calculated to be less than the defined value, highlighting the importance of location for perturbing the system. Numerical results show how optimizing the number and locations of perturbations in a multi-DOFs system can improve the efficiency of the system in term of output harvested power and technological constraints. Reducing the number of transduction circuits allows for considerable development in the size and manufacturing cost of these devices.

Acknowledgments

This work has been supported by the EIPHI Graduate School (contract "ANR-17-EURE-0002")

Appendix A.

The appendix studies the harvested power in a quasi-periodic system of 3-DOFs. Figure A1 shows an equivalent discrete model of a 3-DOF quasi-periodic electromagnetic VEH, subjected to base excitation from ambient vibrations. In order to select the best DOF to perturbed and then harvest energy from it, the criterion of kinetic energy, introduced in

eq. 11, has been calculated for the second and third DOFs. The kinetic energy in case of perturbing the second DOF with an optimal amount of perturbation is almost 60% of total kinetic energy while this amount for the third DOF is below 40%. Therefore, it can be inferred that second DOF is the best location to perturbed. To ensure the consistency of the results, the optimization procedure has also been performed and the second DOF was obtained as the best location, as well.

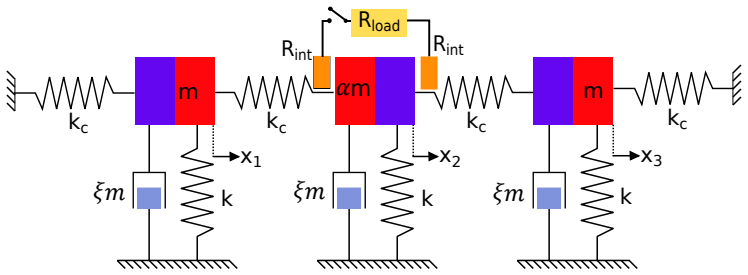

Figure A1: The designed electromagnetic vibration energy harvester

Equations of motion governing the linear behavior of the harvester are expressed as

$$\begin{aligned} \ddot{x}_1 + 2\xi_m\omega_0\dot{x}_1 + \omega_0^2\left[(1+2\beta)\,x_1 - \beta x_2\right] &= -\ddot{X}_g \\ \alpha\ddot{x}_2 + 2\alpha\xi\omega_0\dot{x}_2 + \omega_0^2\left[(1+2\beta)\,x_2 - \beta x_1 - \beta x_3\right] &= -\alpha\ddot{X}_g \\ \ddot{x}_3 + +2\xi_m\omega_0\dot{x}_3 + \omega_0^2\left[(1+2\beta)\,x_3 - \beta x_2\right] &= -\ddot{X}_g \end{aligned} \tag{A.1}$$

in which x is the relative displacement of each DOF and $\ddot{X}_g$ is the basis-imposed acceleration. $\xi = \xi_m + \xi_e$ is the total damping coefficient of the system in which ξ_e and ξ_m are electrical and mechanical damping coefficients, respectively. Moreover, $\beta = K_c/K$ is the coupling coefficient, K is the mechanical stiffness of each DOF and K_c is the coupling linear magnetic stiffness. As discussed, the second mass has been perturbed to confine the energy in it and the electromagnetic transduction is introduced to it through a mechanical-magnetic coupling as follows

$$i(t) = \frac{\delta}{(R_{load} + R_{int})}\dot{x}_2 \tag{A.2}$$

where δ, R_{load} and R_{int} are the electromagnetic coupling coefficient, load resistance, and coil internal resistance, respectively. Considering $x = X(\omega)e^{i\omega t}$ and $u = \omega/\omega_0$, the equations in frequency domain are expressed as

$$ZX = F \tag{A.3}$$

in which

$$Z = \begin{bmatrix} 1+2\beta-u^2+2iu\xi_m & -\beta & 0 \\ -\beta & 1+2\beta-\alpha u^2+2i\alpha u\xi & -\beta \\ 0 & -\beta & 1+2\beta-u^2+2iu\xi_m \end{bmatrix}$$

$$X = \begin{bmatrix} X_1 \\ X_2 \\ X_3 \end{bmatrix}$$

$$F = \begin{bmatrix} -\ddot{X}_g/{\omega_0}^2 \\ -\alpha\ddot{X}_g/{\omega_0}^2 \\ -\ddot{X}_g/{\omega_0}^2 \end{bmatrix} \tag{A.4}$$

The average power, calculated over a cycle of vibration, from the perturbed DOF has been obtained as

$$P_{avr} = \xi_e \alpha m {\omega_0}^3 u^2 |X_2|^2 \tag{A.5}$$

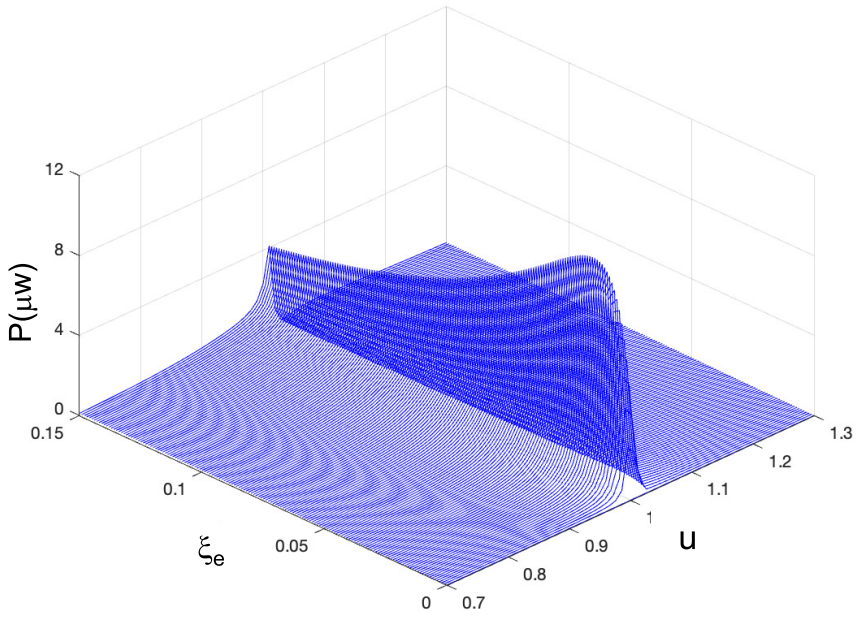

Figure A2: Power magnitude for variations in frequency ratio $u = \omega/\omega_0$ and electrical damping coefficient ξ_e with $\alpha = 1$, $\beta = 0.014$ and $\xi_m = 0.006$

Figures A2 and A3 show the variation in power magnitude with regards to frequency ratio and electrical damping coefficient in $\alpha = 1$ and $\alpha = 1.05$, respectively. It is observed that introducing perturbation increase the harvested power. It has also been shown that harvested power is increasing with the increase in the electrical damping to a specific value. This value of electrical damping is considered as optimal electrical damping.

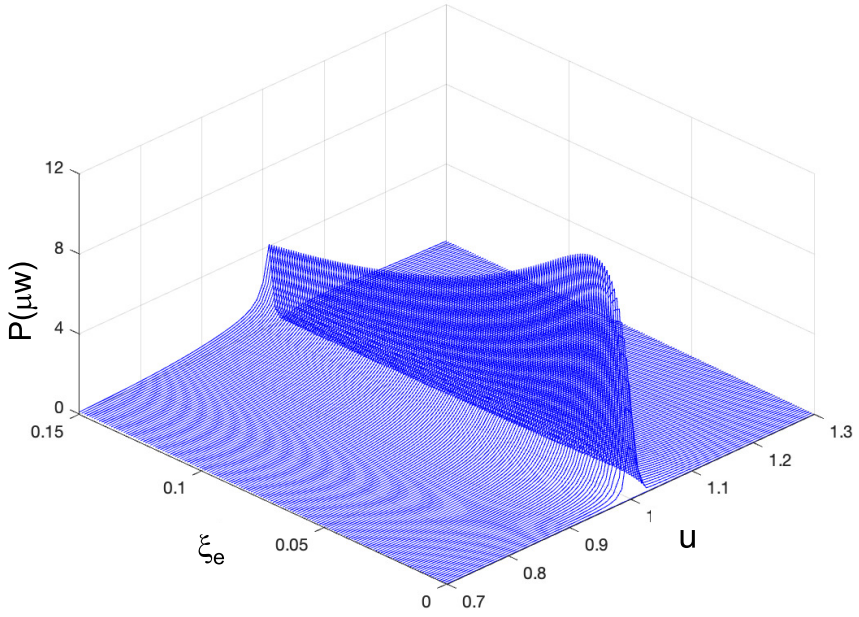

Figure A3: Power magnitude for variations in frequency ratio $u = \omega/\omega_0$ and electrical damping coefficient ξ_e with $\alpha = 1.016$, $\beta = 0.014$ and $\xi_m = 0.006$

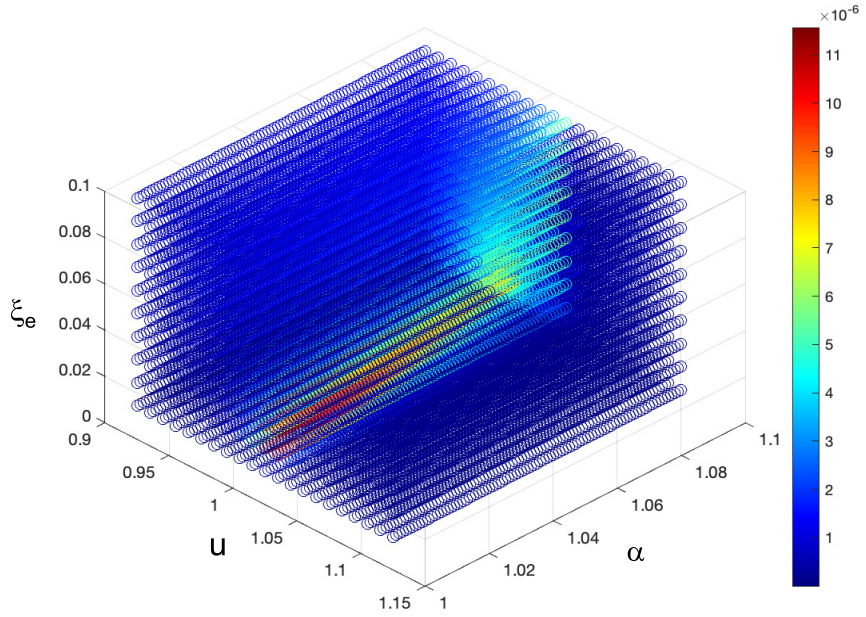

Figure A4: harvested power variations with frequency ratio $u = \omega/\omega_0$ and electrical damping coefficient ξ_e and mass mistuning coefficient α

Figure A4 displays harvested power variations with frequency ratio $u = \omega/\omega_0$, electrical damping coefficient ξ_e and mass mistuning coefficient α. It shows that the harvested power maximizes at a certain range of mass mistuning coefficient value between 1.01 to 1.04 and reaches its highest at α=1.016.

References

[1] Zhao, L., Zou, H., Gao, Q., Yan, G., Wu, Z., Liu, F., Wei, K., Yang, B. & Zhang, W. Design, modeling and experimental investigation of a magnetically modulated rotational energy harvester for low frequency and irregular vibration. *Science China Technological Sciences*. **63**, 2051-2062 (2020)

[2] Zou, H., Zhao, L., Gao, Q., Zuo, L., Liu, F., Tan, T., Wei, K. & Zhang, W. Mechanical modulations for enhancing energy harvesting: Principles, methods and applications. *Applied Energy*. **255** pp. 113871 (2019)

[3] Fortunato, S. Community detection in graphs. *Phys. Rep.-Rev. Sec. Phys. Lett.*. **486** pp. 75-174 (2010)

[4] Khalid, S., Raouf, I., Khan, A., Kim, N. & Kim, H. A review of human-powered energy harvesting for smart electronics: Recent progress and challenges. *International Journal Of Precision Engineering And Manufacturing-Green Technology*. **6**, 821-851 (2019)

[5] Wei, C. & Jing, X. A comprehensive review on vibration energy harvesting: Modelling and realization. *Renewable And Sustainable Energy Reviews*. **74** pp. 1-18 (2017)

[6] Beeby, S., Torah, R., Tudor, M., Glynne-Jones, P., O'donnell, T., Saha, C. & Roy, S. A micro electromagnetic generator for vibration energy harvesting. *Journal Of Micromechanics And Microengineering*. **17**, 1257 (2007)

[7] Sarker, M., Julai, S., Sabri, M., Said, S., Islam, M. & Tahir, M. Review of piezoelectric energy harvesting system and application of optimization techniques to enhance the performance of the harvesting system. *Sensors And Actuators A: Physical*. **300** pp. 111634 (2019)

[8] Zhang, Y., Wang, T., Luo, A., Hu, Y., Li, X. & Wang, F. Micro electrostatic energy harvester with both broad bandwidth and high normalized power density. *Applied Energy*. **212** pp. 362-371 (2018)

[9] Mohanty, A., Parida, S., Behera, R. & Roy, T. Vibration energy harvesting: A review. *Journal Of Advanced Dielectrics*. **9**, 1930001 (2019)

[10] Cassidy, I., Scruggs, J. & Behrens, S. Design of electromagnetic energy harvesters for large-scale structural vibration applications. *Active And Passive Smart Structures And Integrated Systems 2011*. **7977** pp. 79770P (2011)

[11] Fan, K., Liu, S., Liu, H., Zhu, Y., Wang, W. & Zhang, D. Scavenging energy from ultra-low frequency mechanical excitations through a bi-directional hybrid energy harvester. *Applied Energy*. **216** pp. 8-20 (2018)

[12] Yang, B., Lee, C., Kee, W. & Lim, S. Hybrid energy harvester based on piezoelectric and electromagnetic mechanisms. *Journal Of Micro/Nanolithography, MEMS, And MOEMS*. **9**, 023002 (2010)

[13] Vidal, J., Slabov, V., Kholkin, A. & Dos Santos, M. Hybrid Triboelectric-Electromagnetic Nanogenerators for Mechanical Energy Harvesting: A Review. *Nano-Micro Letters*. **13**, 1-58 (2021)

[14] Carneiro, P., Vidal, J., Rolo, P., Peres, I., Ferreira, J., Kholkin, A. & Santos, M. Instrumented electromagnetic generator: Optimized performance by automatic self-adaptation of the generator structure. *Mechanical Systems And Signal Processing*. **171** pp. 108898 (2022)

[15] Lan, C., Chen, Z., Hu, G., Liao, Y. & Qin, W. Achieve frequency-self-tracking energy harvesting using a passively adaptive cantilever beam.*Mechanical Systems And Signal Processing*. **156** pp. 107672 (2021)

[16] Mallick, D., Amann, A. & Roy, S. Surfing the high energy output branch of nonlinear energy harvesters. *Physical Review Letters*. **117**, 197701 (2016)

[17] Tehrani, M. & Elliott, S. Extending the dynamic range of an energy harvester using nonlinear damping. *Journal Of Sound And Vibration*. **333**, 623-629 (2014)

[18] Daqaq, M., Masana, R., Erturk, A. & Dane Quinn, D. On the role of nonlinearities in vibratory energy harvesting: a critical review and discussion. *Applied Mechanics Reviews*. **66** (2014)

[19] Izadgoshasb, I., Lim, Y., Vasquez Padilla, R., Sedighi, M. & Novak, J. Performance enhancement

of a multiresonant piezoelectric energy harvester for low frequency vibrations. *Energies*. **12**, 2770 (2019)

[20] Santos, M., Ferreira, J., Simões, J., Pascoal, R., Torrão, J., Xue, X. & Furlani, E. Magnetic levitation-based electromagnetic energy harvesting: a semi-analytical non-linear model for energy transduction. *Scientific Reports*. **6**, 1-9 (2016)

[21] Abed, I., Kacem, N., Bouhaddi, N. & Bouazizi, M. Multi-modal vibration energy harvesting approach based on nonlinear oscillator arrays under magnetic levitation. *Smart Materials And Structures*. **25**, 025018 (2016)

[22] Zergoune, Z., Kacem, N. & Bouhaddi, N. On the energy localization in weakly-coupled oscillators for electromagnetic vibration energy harvesting. *Smart Materials And Structures*. **28**, 07LT02 (2019)

[23] Aouali, K., Kacem, N., Bouhaddi, N., Mrabet, E. & Haddar, M. Efficient broadband vibration energy harvesting based on tuned non-linearity and energy localization. *Smart Materials And Structures*. **29**, 10LT01 (2020)

[24] Pierre, C. Weak and strong vibration localization in disordered structures: a statistical investigation. *Journal Of Sound And Vibration*. **139**, 111-132 (1990)

[25] Anderson, P. Absence of diffusion in certain random lattices. *Physical Review*. **109**, 1492 (1958)

[26] Stephen, N. On energy harvesting from ambient vibration. *Journal Of Sound And Vibration*. **293**, 409-425 (2006)

[27] Saleem, U., Qureshi, H., Jangsher, S. & Saleem, M. Transmission power management for throughput maximization in harvesting enabled D2D network. *2016 IEEE Symposium On Computers And Communication (ISCC)*. pp. 1078-1083 (2016)

[28] Homayouni-Amlashi, A., Schlinquer, T., Mohand-Ousaid, A. & Rakotondrabe, M. 2D topology optimization MATLAB codes for piezoelectric actuators and energy harvesters. *Structural And Multidisciplinary Optimization*. **63**, 983-1014 (2021)

[29] Jiang, T., Zhang, L., Chen, X., Han, C., Tang, W., Zhang, C., Xu, L. & Wang, Z. Structural optimization of triboelectric nanogenerator for harvesting water wave energy. *ACS Nano*. **9**, 12562-12572 (2015)

[30] Homayouni-Amlashi, A., Mohand-Ousaid, A. & Rakotondrabe, M. Analytical modelling and optimization of a piezoelectric cantilever energy harvester with in-span attachment. *Micromachines*. **11**, 591 (2020)

[31] Flankl, M., Tüysüz, A. & Kolar, J. Cogging torque shape optimization of an integrated generator for electromechanical energy harvesting. *IEEE Transactions On Industrial Electronics*. **64**, 9806-9814 (2017)

[32] Mohajer, N. & Mahjoob, M. Modeling and electrical optimization of a designed Piezoelectric-based vibration Energy Harvesting System. *2013 First RSI/ISM International Conference On Robotics And Mechatronics (ICRoM)*. pp. 455-461 (2013)

[33] Abed, I., Kacem, N., Bouhaddi, N. & Bouazizi, M. Optimized nonlinear mdof vibration energy harvester based on electromagnetic coupling. *International Conference Design And Modeling Of Mechanical Systems*. pp. 31-38 (2017)

[34] Aouali, K., Kacem, N., Bouhaddi, N. & Haddar, M. On the Optimization of a Multimodal Electromagnetic Vibration Energy Harvester Using Mode Localization and Nonlinear Dynamics. *Actuators*. **10**, 25 (2021)

[35] Lampinen, J. & Zelinka, I. Mixed integer-discrete-continuous optimization by differential evolution. *Proceedings Of The 5th International Conference On Soft Computing*. pp. 71-76 (1999)

[36] Marler, R. & Arora, J. The weighted sum method for multi-objective optimization: new insights. *Structural And Multidisciplinary Optimization*. **41**, 853-862 (2010)

[37] Grodzevich, O. & Romanko, O. Normalization and other topics in multi-objective optimization. (2006)

[38] Sivanandam, S. & Deepa, S. Genetic algorithms. *Introduction To Genetic Algorithms*. pp. 15-37 (2008)

[39] Ashraf, K., Khir, M., Dennis, J. & Baharudin, Z. A wideband, frequency up-converting bounded vibration energy harvester for a low-frequency environment. *Smart Materials And Structures*. **22**, 025018 (2013)

[40] Liu, W., Badel, A., Formosa, F., Wu, Y. & Agbossou, A. Novel piezoelectric bistable oscillator architecture for wideband vibration energy harvesting. *Smart Materials And Structures*. **22**, 035013 (2013)

[41] Mann, B. & Owens, B. Investigations of a nonlinear energy harvester with a bistable potential well. *Journal Of Sound And Vibration*. **329**, 1215-1226 (2010)

[42] Beato-López, J., Royo-Silvestre, I., Algueta-Miguel, J. & Gomez-Polo, C. A combination of a vibrational electromagnetic energy harvester and a giant magnetoimpedance (GMI) sensor. *Sensors*. **20**, 1873 (2020)

[43] Saravia, C., Ramırez, J. & Gatti, C. A hybrid numerical-analytical approach for modeling levitation based vibration energy harvesters. *Sensors And Actuators A: Physical*. **257** pp. 20-29 (2017)

[44] Zhao, X., Cai, J., Guo, Y., Li, C., Wang, J. & Zheng, H. Modeling and experimental investigation of an AA-sized electromagnetic generator for harvesting energy from human motion. *Smart Materials And Structures*. (2018)

[45] Drezet, C., Kacem, N. & Bouhaddi, N. Design of a nonlinear energy harvester based on high static low dynamic stiffness for low frequency random vibrations.*Sensors And Actuators A: Physical*. **283** pp. 54-64 (2018)